Geomorphology 186 (2013) 39–49

Contents lists available at SciVerse ScienceDirect

Geomorphology

journal homepage: www.elsevier.com/locate/geomorph

Application of the topographic position index to heterogeneous landscapes

Jeroen De Reu [a,*], Jean Bourgeois [a], Machteld Bats [a], Ann Zwertvaegher [b], Vanessa Gelorini [b], Philippe De Smedt [c], Wei Chu [e], Marc Antrop [d], Philippe De Maeyer [d], Peter Finke [b], Marc Van Meirvenne [c], Jacques Verniers [b], Philippe Crombé [a]

[a] Department of Archaeology, Ghent University, Sint-Pietersnieuwstraat 35, 9000 Ghent, Belgium
[b] Department of Geology and Soil Science, Ghent University, Krijgslaan 281, 9000 Ghent, Belgium
[c] Department of Soil Management, Ghent University, Coupure 653, 9000 Ghent, Belgium
[d] Department of Geography, Ghent University, Krijgslaan 281, 9000 Ghent, Belgium
[e] Department of Archaeology, University of Reading, Whiteknights, Reading RG6 6AB, Berks, United Kingdom

ARTICLE INFO

Article history:
Received 10 October 2011
Received in revised form 30 November 2012
Accepted 15 December 2012
Available online 22 December 2012

Keywords:
Digital elevation model
Geomorphometry
Topographic position index
Deviation from mean elevation
Slope position classification
Landform classification

ABSTRACT

Topographic position index (*TPI*) is an algorithm increasingly used to measure topographic slope positions and to automate landform classifications. We applied *TPI* to a geoarchaeological research project in northwestern Belgium but its use led to erroneous landform classifications in this heterogeneous landscape. We asked whether deviation from mean elevation (*DEV*) was a better method for landform classification than *TPI*. We found that it enabled more accurate geomorphological assessment when using northwestern Belgium as a case study.

© 2012 Elsevier B.V. All rights reserved.

1. Introduction

Over the last decade, geographical information systems (GIS) and digital elevation models (DEMs) have been increasingly used to automatically classify landforms (Burrough et al., 2000; Drăguţ and Blaschke, 2006; Iwahashi and Pike, 2007; Hengl and Reuter, 2009). Disparate techniques incorporate a range of topographic input variables and output a varying number of landform classes (e.g. Irvin et al., 1997; Giles, 1998; Miliaresis and Argialas, 1999; MacMillan et al., 2000, 2004; Hengl and Rossiter, 2003; Bolongaro-Crevenna et al., 2005; Prima et al., 2006). These techniques have been applied to earth surfaces, ocean floors (e.g. Wright and Heyman, 2008; Zieger et al., 2009), and planets (e.g. Bue and Stepinski, 2006). However, Drăguţ and Blaschke (2006) assert that geomorphometric classifications of terrains have focused on either homogeneous regions (Schmidt and Dikau, 1999; MacMillan et al., 2000) or specific features such as hills, mountains (e.g. Miliaresis and Argialas, 1999) and hillslope units (e.g. Irvin et al., 1997; Burrough et al., 2000; MacMillan et al., 2000), thereby making heterogenous landscapes less studied. Additionally, Pike et al. (2009) remarked that no DEM-derived map is definitive, as the parameters can be generated by different algorithms or sampling strategies and can vary with spatial scale.

Following Guisan et al. (1999), Weiss (2001) introduced a customised GIS application for semi-automated landform classification; the so-called topographic position index (*TPI*) or difference from mean elevation (*DIFF*) as defined by Gallant and Wilson (2000). *TPI* measures the relative topographic position of the central point as the difference between the elevation at this point and the mean elevation within a predetermined neighbourhood. Using *TPI*, landscapes can be classified in slope position classes. *TPI* is only one of a vast array of morphometric properties based on neighbouring areas that can be useful in topographic and DEM analysis (see Gallant and Wilson, 2000).

Since the creation of an ESRI ArcView 3.x extension by Jenness (2006), *TPI* has been applied to the fields of geomorphology (Tagil and Jenness, 2008; Liu et al., 2009; McGarigal et al., 2009); geology (Mora-Vallejo et al., 2008; Deumlich et al., 2010; Illés et al., 2011); hydrology (Lesschen et al., 2007; Francés and Lubczynski, 2011; Liu et al., 2011); agricultural science (Pracilio et al., 2006); behavioural ecology (Coulon et al., 2008; Podchong et al., 2009; de la Giroday et al., 2011); forest management (Fei et al., 2007; Zhang et al., 2009; Giorgis et al., 2011; Han et al., 2011; Weber, 2011; Clark et al., 2012); wildlife management (Squires et al., 2008; Lacki et al., 2009; Pinard et al., 2012); climatology (Etienne et al., 2010; Bunn et al., 2011); archaeology (Patterson, 2008; Berking et al., 2010); health care (Clennon et al., 2010; Moss et al., 2011) and risk management (Platt et al., 2011; Wood et al., 2011). Additionally, the bathymetric position index (*BPI*), which is derived from *TPI*, is frequently used in

* Corresponding author. Tel.: +32 93310155; fax: +32 93310297.
E-mail address: Jeroen.DeReu@UGent.be (J. De Reu).

0169-555X/$ – see front matter © 2012 Elsevier B.V. All rights reserved.
http://dx.doi.org/10.1016/j.geomorph.2012.12.015

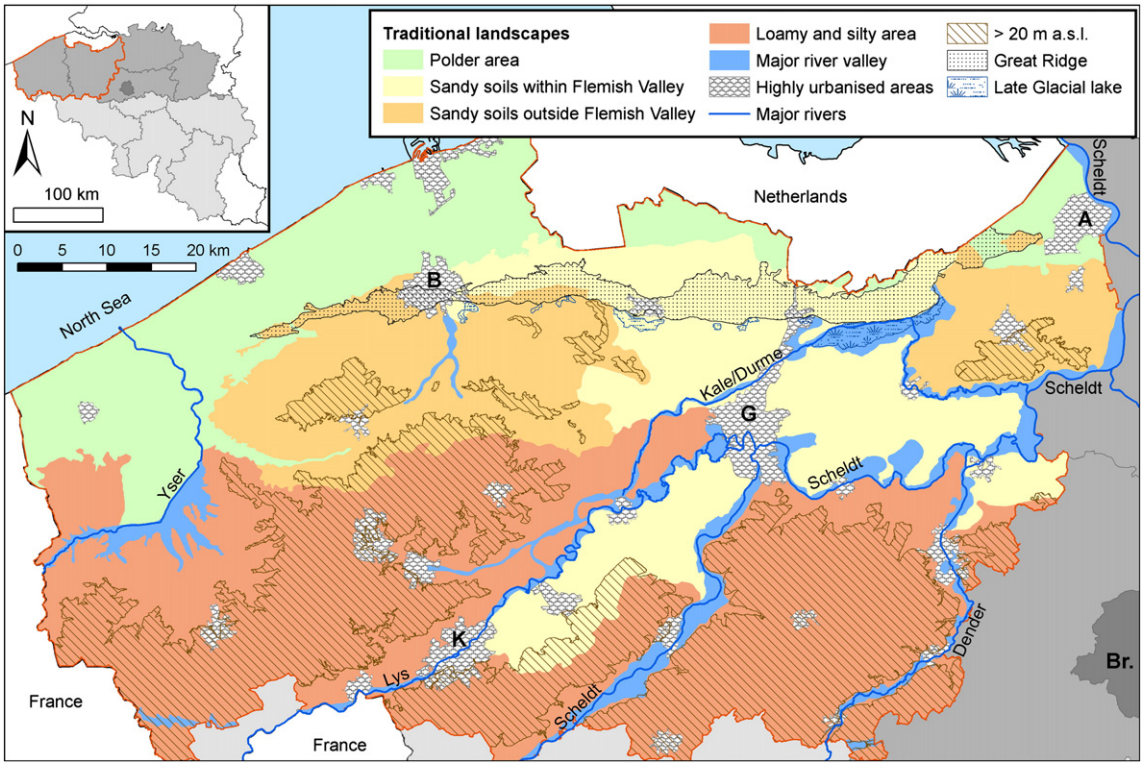

Fig. 1. Map of northwestern Belgium showing main landscape units (major cities: A: Antwerp, B: Bruges, Br. Brussels, G: Ghent and K: Kortrijk).

seafloor mapping (e.g. Iampietro et al., 2005; Lundblad et al., 2006; Verfaillie et al., 2006; Wilson et al., 2007; Wright and Heyman, 2008; Zieger et al., 2009; Young et al., 2011).

Given *TPI*'s ability to subdivide landscapes into morphological classes based on topography, the method is important for archaeological landscape research, aiming to identifying the topographic preference

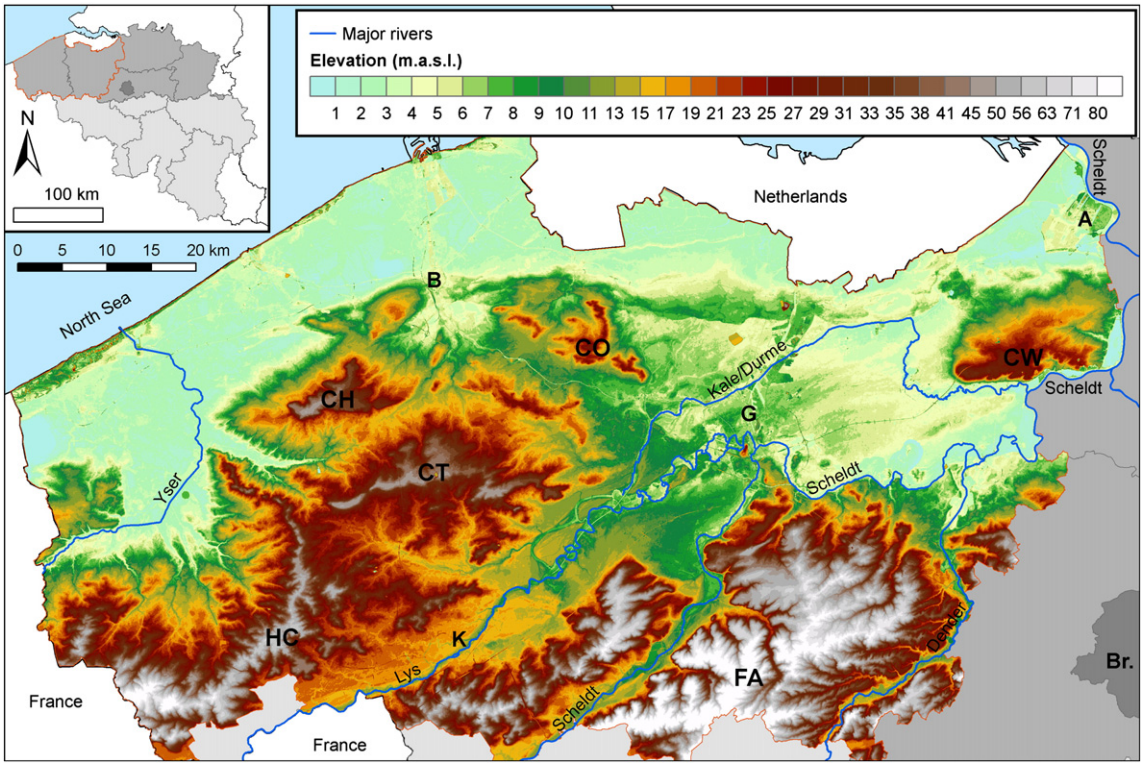

Fig. 2. DEM of northwestern Belgium (cuestas: CH: Hertsberghe, CO: Oedelem, CT: Tielt and CW: Land van Waas; hilly regions: FA: Flemish Ardennes and HC: hills of Central West Flanders; major cities: A: Antwerp, B: Bruges, Br. Brussels, G: Ghent and K: Kortrijk).

Table 1
Classification of the landscape into slope position classes.

Morphologic class	Weiss (2001)	Northwestern Belgium
Ridge	$z_0 > SD$	$z_0 > SD$
Upper slope	$SD \geq z_0 > 0.5SD$	$SD \geq z_0 > 0.5SD$
Middle slope	$0.5SD \geq z_0 \geq -0.5SD$, slope $> 5°$	Pos. values: $0.5SD \geq z_0 \geq 0$
Flat area	$0.5SD \geq z_0 \geq -0.5SD$, slope $\leq 5°$	Neg. values: $0 > z_0 \geq -0.5SD$
Lower slope	$-0.5SD > z_0 \geq -SD$	$-0.5SD > z_0 \geq -SD$
Valley	$z_0 < -SD$	$z_0 < -SD$

of specific types of archaeological sites (e.g. settlement and burial sites). Indeed, local topography and topographic positions are often described as important parameters determining the location of an archaeological site (e.g. Tilley, 1994). However, most archaeologists do not apply analytical tools such as GIS to assess the relationship, and interpretations are mostly based on their observations and experiences. Notable exceptions can be found in the work of Kvamme (1992), Warren and Asch (2000), Llobera (2001), Roughley (2001), Bevan (2002), Christopherson (2003), Bevan and Conolly (2004) and Fairén-Jiménez (2007).

In a geoarchaeological research project in northwestern Belgium, *TPI* was used to analyse the topographic location of prehistoric settlements (Crombé et al., 2011) and Bronze Age burial mounds (De Reu et al., 2011). However, the results based on the landform classification method of Weiss (2001) did not correspond to real topography. This was due to the complex heterogeneous shape of the landscape under investigation. This paper discusses *TPI* and its limitations in a study area of northwestern Belgium. An additional parameter, the deviation from mean elevation (*DEV*), is assessed to improve the classifications of slope positions and landforms.

2. Study area

The study area is situated in the provinces of East and West Flanders, northwestern Belgium. The area can be subdivided into three traditional landscape units: (i) the sandy area (Sandy Flanders), (ii) the polder area and (iii) the loamy and silty area (Fig. 1). The central part of Sandy Flanders is the Flemish Valley (Fig. 2), a Pleistocene valley formed by successive periods of fluvial incision and infilling during glacial and interglacial periods (De Moor and Heyse, 1978; Heyse, 1979). It is a low-lying area, mainly covered with sandy sediments that rarely exceed heights above 10 m and vary by a few metres. Although it is considered flat, the general topography is characterised by a subtle topography composed of hundreds of small, low and elongated ridges, shallow depressions and stream valleys. One ridge, the so-called Great Ridge, rises up to 5 m above the surrounding landscape. Towards the east and the west, the Flemish Valley is enclosed by cuestas, Tertiary outcrops as high as 30 m. Sandy Flanders is bordered to the north and west by the polder area, an expanse covered with marine and alluvial sediments of the coastal polders and the polders of the River Scheldt. Towards the south, Sandy Flanders is bordered by the loamy and silty area, topographically characterised by the hills of Central West Flanders and the Flemish Ardennes, with heights up to 150 m. This region is incised by streams of varying size throughout.

3. Material and methods

3.1. Elevation data

A DEM based on high-density airborne LiDAR (light detection and ranging) data registered between 2001 and 2004, was used for the whole study area (Fig. 2) (AGIV, 2003; Werbrouck et al., 2011). The data were generated in grid formats with cell sizes of 5, 25 and 100 m through the inverse distance weighting (IDW) interpolation. In this study, the 5 m DEM was used, where vegetation and buildings are filtered before delivery (AGIV, 2004). Other artificial structures such as road banks and waste dumps were not filtered (Werbrouck et al., 2011).

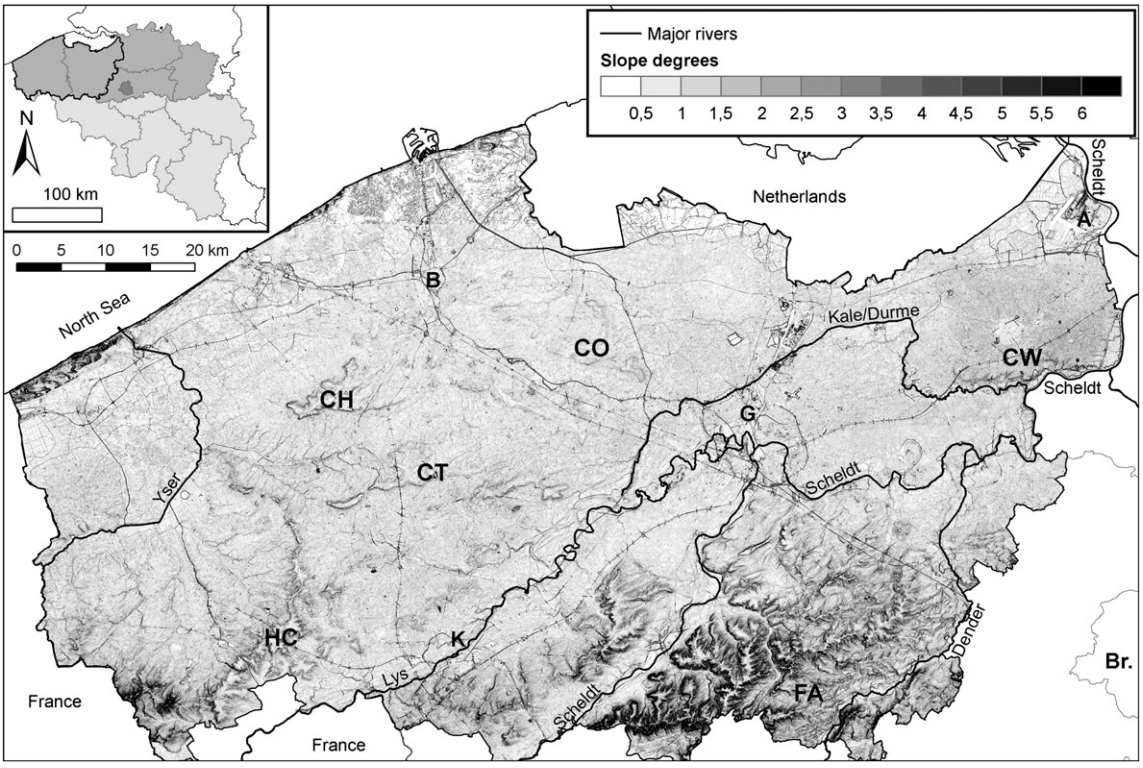

Fig. 3. DEM-derived slope map of northwestern Belgium (cuestas: CH: Hertsberghe, CO: Oedelem, CT: Tielt and CW: Land van Waas; hilly regions: FA: Flemish Ardennes and HC: hills of Central West Flanders; major cities: A: Antwerp, B: Bruges, Br. Brussels, G: Ghent and K: Kortrijk).

Table 2
Classification of the landscape into landform classes.
After Weiss (2001).

Landform	Small neighbourhood size	Large neighbourhood size
(1) Deeply incised streams	$z_0 < -SD$	$z_0 < -SD$
(2) Local valley in plain	$z_0 < -SD$	$-SD \le z_0 < 0$
(3) Middle slope drainage	$z_0 < -SD$	$0 \le z_0 \le SD$
(4) Upland drainage	$z_0 < -SD$	$z_0 > SD$
(5) U-shape valleys	$-SD \le z_0 \le SD$	$z_0 < -SD$
(6) Open slopes, flat areas ($LNS < 0$)	$-SD \le z_0 \le SD$	$-SD \le z_0 < 0$
(7) Open slopes, flat areas ($LNS \ge 0$)	$-SD \le z_0 \le SD$	$0 \le z_0 \le SD$
(8) Upper slopes	$-SD \le z_0 \le SD$	$z_0 > SD$
(9) Local hills/ridges in valley	$z_0 > SD$	$z_0 < -SD$
(10) Local hills/ridges in plain	$z_0 > SD$	$-SD \le z_0 < 0$
(11) Middle slope ridges	$z_0 > SD$	$0 \le z_0 \le SD$
(12) Hill tops, high ridges	$z_0 > SD$	$z_0 > D$

3.2. TPI

TPI measures the difference between elevation at the central point (z_0) and the average elevation ($\bar{z}$) around it within a predetermined radius (R) (Gallant and Wilson, 2000; Weiss, 2001):

$$TPI = z_0 - \bar{z} \tag{1}$$

$$\bar{z} = \frac{1}{n_R} \sum_{i \in R} z_i. \tag{2}$$

Positive *TPI* values indicate that the central point is located higher than its average surroundings, while negative values indicate a position lower than the average. The range of *TPI* depends not only on elevation differences but also on R (e.g. Grohmann and Riccomini, 2009). Large R-values mainly reveal major landscape units, while smaller values highlight smaller features, such as minor valleys and ridges.

3.3. DEV

DEV measures the topographic position of the central point (z_0) using *TPI* and the standard deviation of the elevation (SD) (Gallant and Wilson, 2000):

$$DEV = \frac{z_0 - \bar{z}}{SD} \tag{3}$$

$$SD = \sqrt{\frac{1}{n_R - 1} \sum_{i=1} (z_i - \bar{z})^2}. \tag{4}$$

DEV measures the topographic position as a fraction of local relief normalised to local surface roughness. Again, the output value is

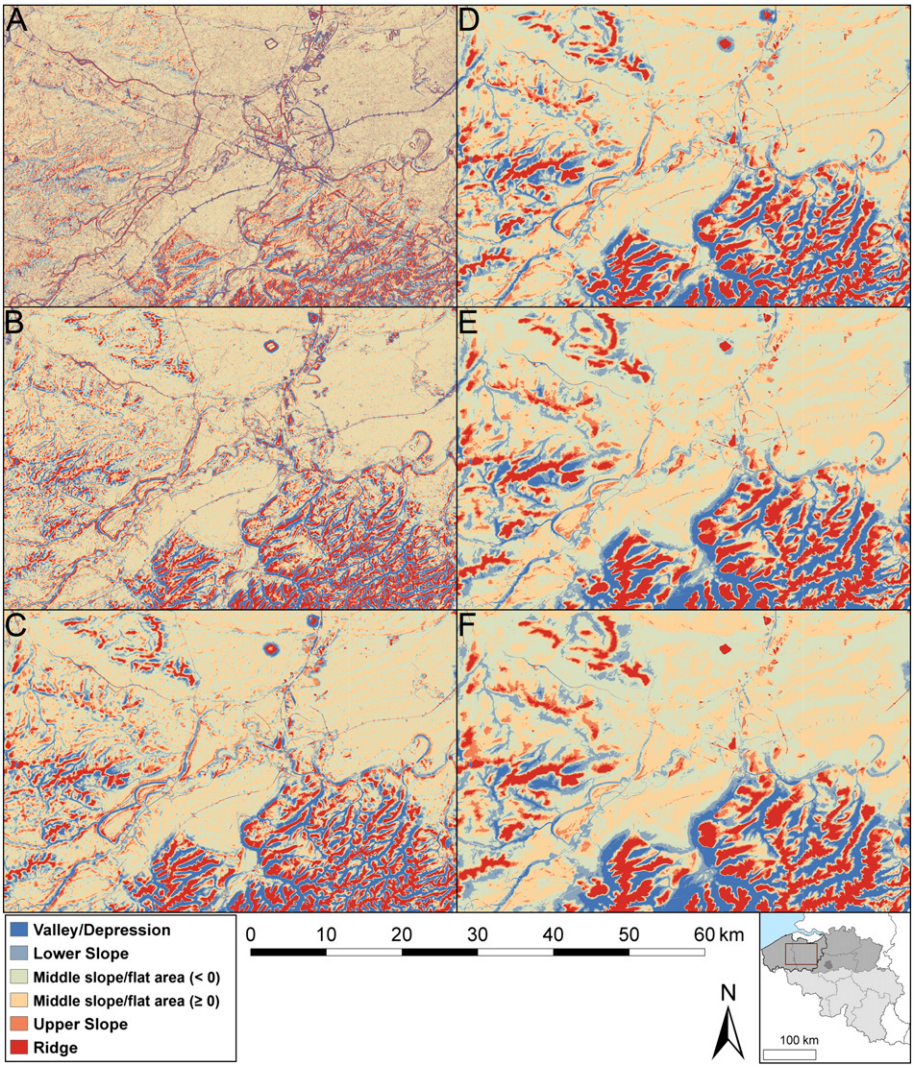

Fig. 4. Slope position classification based on *TPI* for (A) 100 m, (B) 300 m, (C) 600 m, (D) 1000 m, (E) 1500 m and (F) 2000 m neighbourhood sizes.

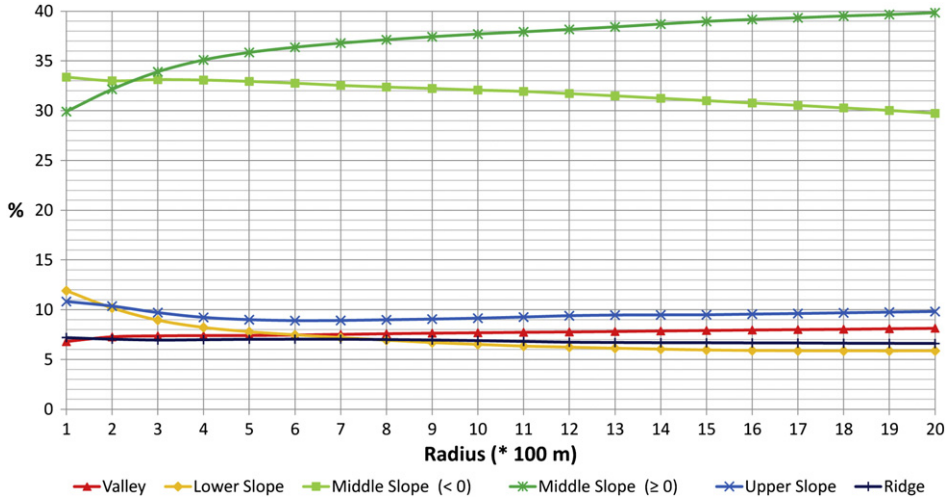

Fig. 5. Percentages of the slope position classes based on *TPI* for different neighbourhood sizes.

positive when the central point is situated higher than its neighbourhood and negative when it is situated lower. The output values mostly range between +1 and −1, and values outside this range may indicate anomalies within the DEM.

3.4. Landform classification

There are a wide range of geomorphological methods and algorithms to classify the landscape into morphological classes (e.g. Burrough et al., 2000; Deng, 2007; Iwahashi and Pike, 2007; Hengl and Reuter, 2009). We applied the method of Weiss (2001) that classifies the landscape into discrete slope position classes using the standard deviation of *TPI*. Six classes were defined using the criteria shown in Table 1. In applying the method of Weiss (2001), threshold values to distinguish slopes different from the original have been frequently used (e.g. Tagil and Jenness, 2008; Deumlich et al., 2010). For the study area, flat areas and middle slopes were not differentiated, as large slope values only appear in a small part of the study area (Flemish Ardennes; Fig. 3). We distinguished between middle slopes/flat areas that are higher than their surroundings ($TPI/DEV \geq 0$) and those that are lower than their surroundings ($TPI/DEV < 0$).

In addition, the parameters from two neighbourhood sizes are combined in order to identify complex landscape features, because such a combination provides more information about topography (Weiss, 2001). Table 2 summarises 12 produced landform classes.

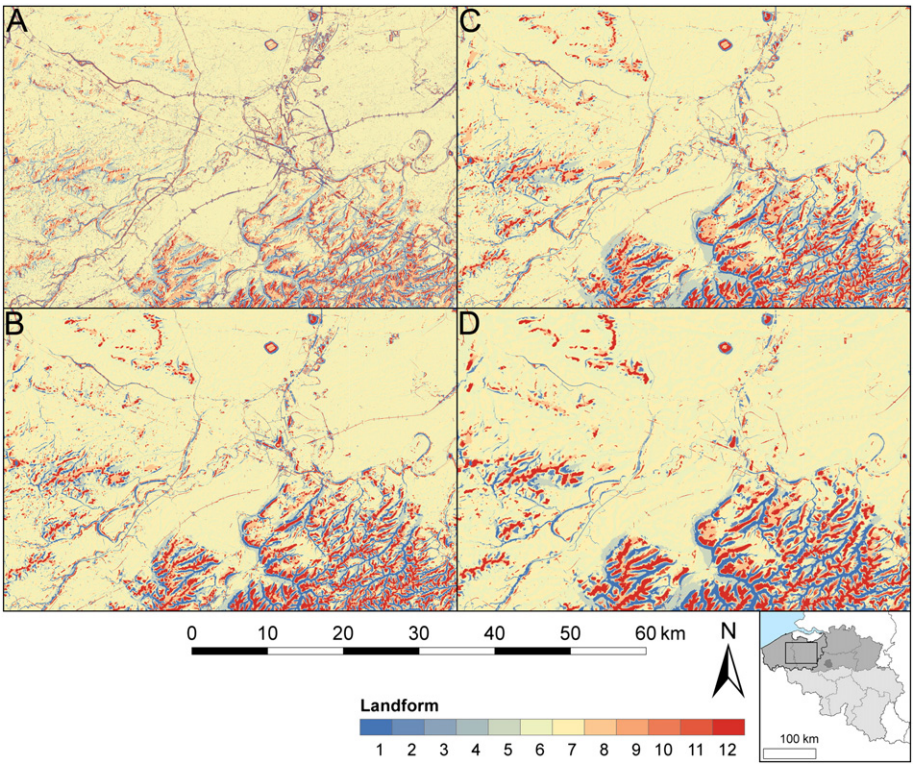

Fig. 6. Landform classification based on *TPI* for combined neighbourhood sizes: (A) 100 and 600 m, (B) 300 and 1000 m, (C) 300 and 2000 m and (D) 600 and 2000 m. The description of the landforms is in Table 2.

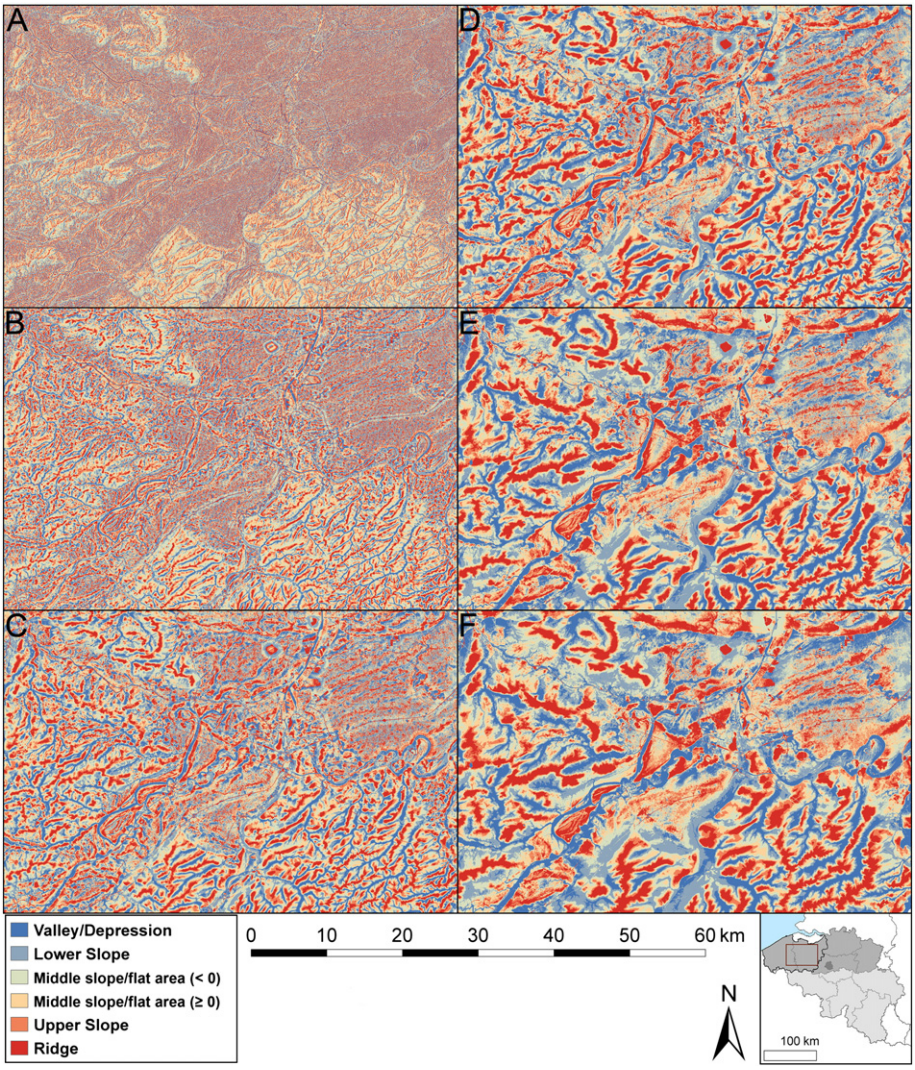

Fig. 7. Slope position classification based on *DEV* for (A) 100 m, (B) 300 m, (C) 600 m, (D) 1000 m, (E) 1500 m and (F) 2000 m neighbourhood sizes.

3.5. Data processing and neighbourhood size

TPI and *DEV* were calculated using the focal operators of ESRI's ArcGIS 9.3 and by using Reuter's ArcGIS script elevres.aml (Reuter and Nelson, 2009). For both *TPI* and *DEV*, the most insightful neighbourhood sizes were identified from 20 candidate radii from 100 to 2000 m with a 100 m interval. Results for six neighbourhood sizes (100, 300, 600, 1000, 1500 and 2000 m) are presented in this paper.

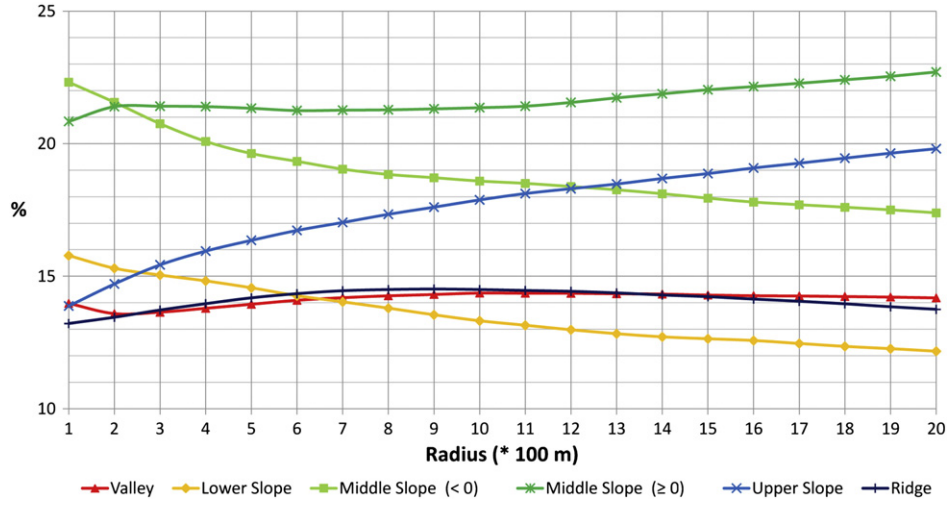

Fig. 8. Percentages of the slope position based on *DEV* for different neighbourhood sizes.

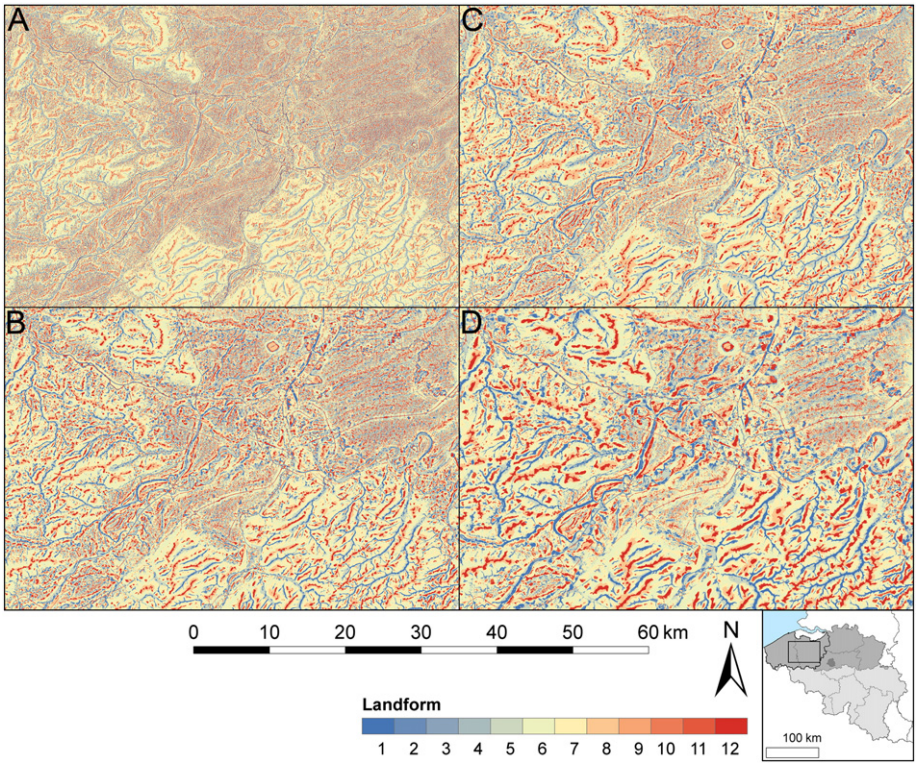

Fig. 9. Landform classification based on *DEV* for combined neighbourhood sizes: (A) 100 and 600 m, (B) 300 and 1000 m, (C) 300 and 2000 m and (D) 600 and 2000 m. The description of the landforms is in Table 2.

4. Results

The generated *TPI* maps (Fig. 4) showed the influence of neighbourhood size on the landform classifications; smaller radii better represented small features. Fig. 5 illustrates the percentage of the slope position classes for each radius. The middle slope/flat area was the largest category, with percentages ranging between 63.28% (100 m) and 69.97% (1500 m). Each of the other four categories (valley, lower slope, upper slope and ridge) represented between 5% and 10%. However, for all neighbourhood sizes, the distribution of these classes was mainly related to the extent of certain landscape features (Figs. 2 and 4). The category ridge was often associated with the higher parts of the Tertiary cuestas and the hills in Central West Flanders and the Flemish Ardennes. Also the category valley was almost only identified in these more hilly regions, where it can be associated with deeper incised streams, and in the major river valleys of the Scheldt and the Lys. The area in and around the Flemish Valley was largely identified as middle slope/flat area. The subtle topography characteristic for this area was not recognised. For example, the small, elongated sand ridges along small stream valleys were either unidentified or only to a very limited extent. As such, the results were unsatisfactory, as they did not correspond to actual topography. Moreover, the combination of two neighbourhood sizes provided no significant outcome (Fig. 6).

The generated *DEV* maps (Fig. 7) also showed the influence of neighbourhood size. Fig. 8 illustrates the percentage of the slope position classes for different radii, showing a pattern considerably different from the *TPI* classification. Each class comprises 12% to 23% of the area, and their trend was influenced by neighbourhood size. The most variable classes were the upper slope, increasing from 13.88% (100 m) to 19.81% (2000 m), and the middle slope/flat area ($TPI<0$), decreasing from 22.32% (100 m) to 17.39% (2000 m). The most stable classes were ridges and valleys, both ranging between 13.25% and 14.50%. Despite these variations, the generated output corresponded more with the local topographic reality because more landscape features were recognised. Ridges and valleys were also recognised in the subtle topography of the Flemish Valley, where these correspond to elongated sand ridges and valleys in between. Also in the areas around the Tertiary cuestas and the hills of Central West Flanders and the Flemish Ardennes, the result was more realistic. Ridges correspond to the crests of hills, while valleys were only assigned to the lowest areas between the ridges. Upper slopes, middle slope/flat areas and lower slopes were more accurately recognised. Similar results were obtained when different neighbourhood sizes were combined (Fig. 9).

The more accurate assessment of landforms using *DEV* instead of *TPI* was also conducted based on the relation between the soil drainage classes and slope position classes. The drainage classes were derived from the digital soil map of Flanders (AGIV, 2001) and grouped in four categories: dry, moderately dry, moderately wet, and wet. The distribution of classes for each slope position class was then analysed. Fig. 10 shows that the distribution is similar between *DEV* and *TPI*. The wet soil was overrepresented in the valleys, depressions and the lower slope areas, while underrepresentation occurred in higher areas particularly on the middle slopes/flat areas ($TPI/DEV \geq 0$), the upper slopes and the ridges. The dry ground showed a reverse distribution: overrepresentation on the ridges and upper slopes and underrepresentation in lower areas particularly the middle slopes/flat areas ($TPI/DEV<0$), lower slopes, valleys and depressions.

However, if the spatial relation between the soil drainage classes and slope position classes is considered, large differences between *TPI* and *DEV* were observed. Fig. 11 shows the correlation between the wet soils along valleys and depressions as well as on lower slopes, and that between dry soils on ridges and upper slopes. When *TPI* was used, correlations between the drainage and slope classes were shown only in the hilly regions around the hills of Central West Flanders and the Flemish Ardennes. If *DEV* was used, correlations appear in the whole study area, which is more realistic. The comparison of the present-day hydrological network and the generated slope classes (Fig. 11) also illustrated a more accurate classification using *DEV*.

5. Discussion and conclusions

TPI, as defined by Weiss (2001), proved to be a useful tool for classifying slope positions and landforms. This was previously illustrated by Weiss (2001) for Mt Hood in Oregon, USA, and Tagil and Jenness (2008) for the Yazoren Polje, Turkey. However, both regions have relatively homogeneous landscapes (Drăguţ and Blaschke, 2006) with similar landforms (i.e. mountains and deep valleys). Our study in northwestern Belgium illustrates the shortcomings of *TPI* for complex landscapes characterised by a combination of (i) subtle landforms with height differences of only a few metres (Flemish Valley) and (ii) a more pronounced topography around the Tertiary outcrops and the hills of Central West Flanders and the Flemish Ardennes, with height differences of several metres or more. The range of *TPI* is strongly influenced by surface roughness, which resulted in an incorrect classification of slope positions and landforms in these complex and heterogeneous landscapes. To reduce the influence of the surface roughness on the detection of slope classes at the local scale, *DEV* was applied. This allowed us to analyse the heterogeneous landscapes more accurately, and prominent locations, flat areas and

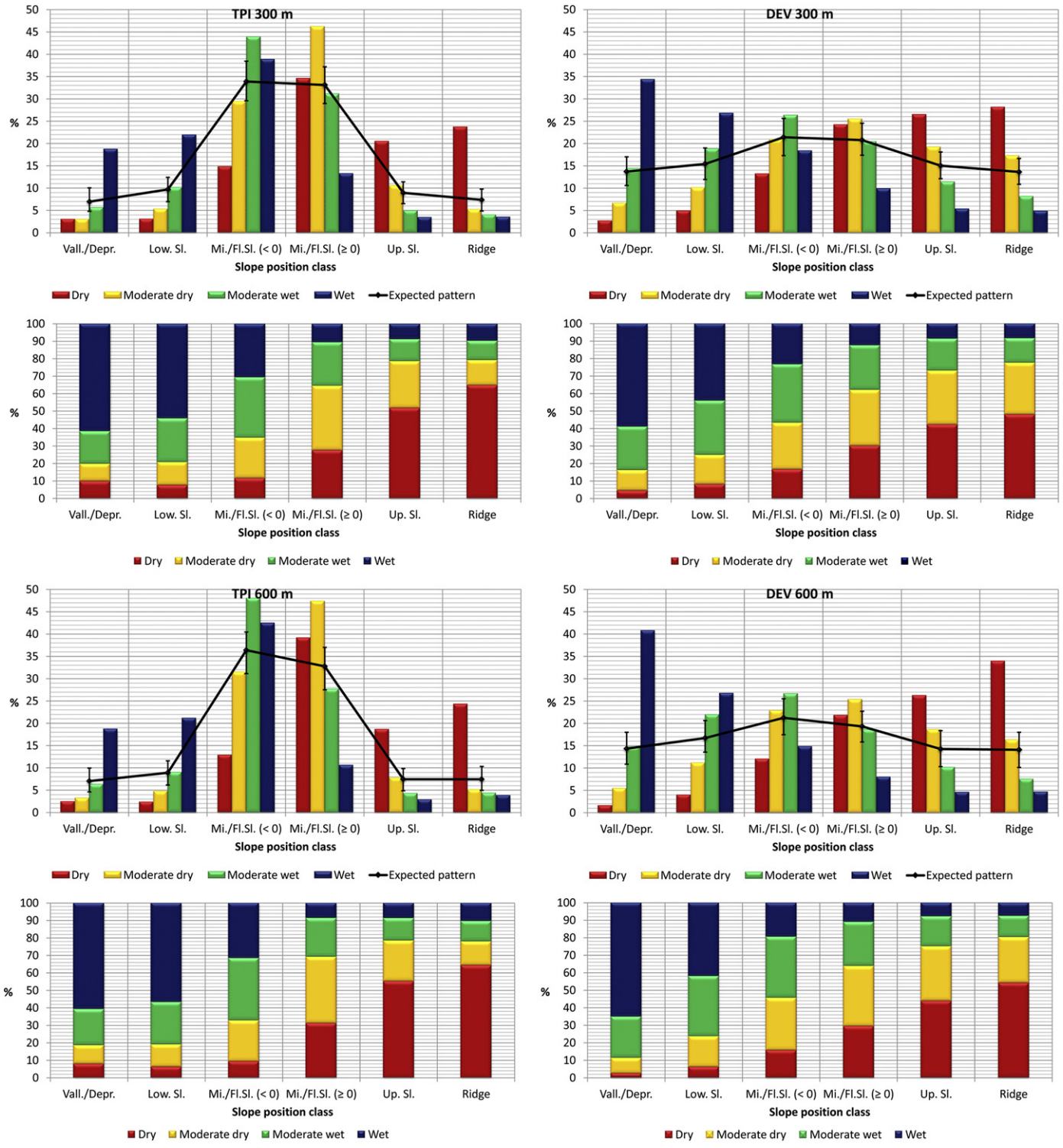

Fig. 10. Percentages of the drainage classes based on *DEV* or *TPI* for different slope position classes and neighbourhood size (300, 600 and 1000 m).

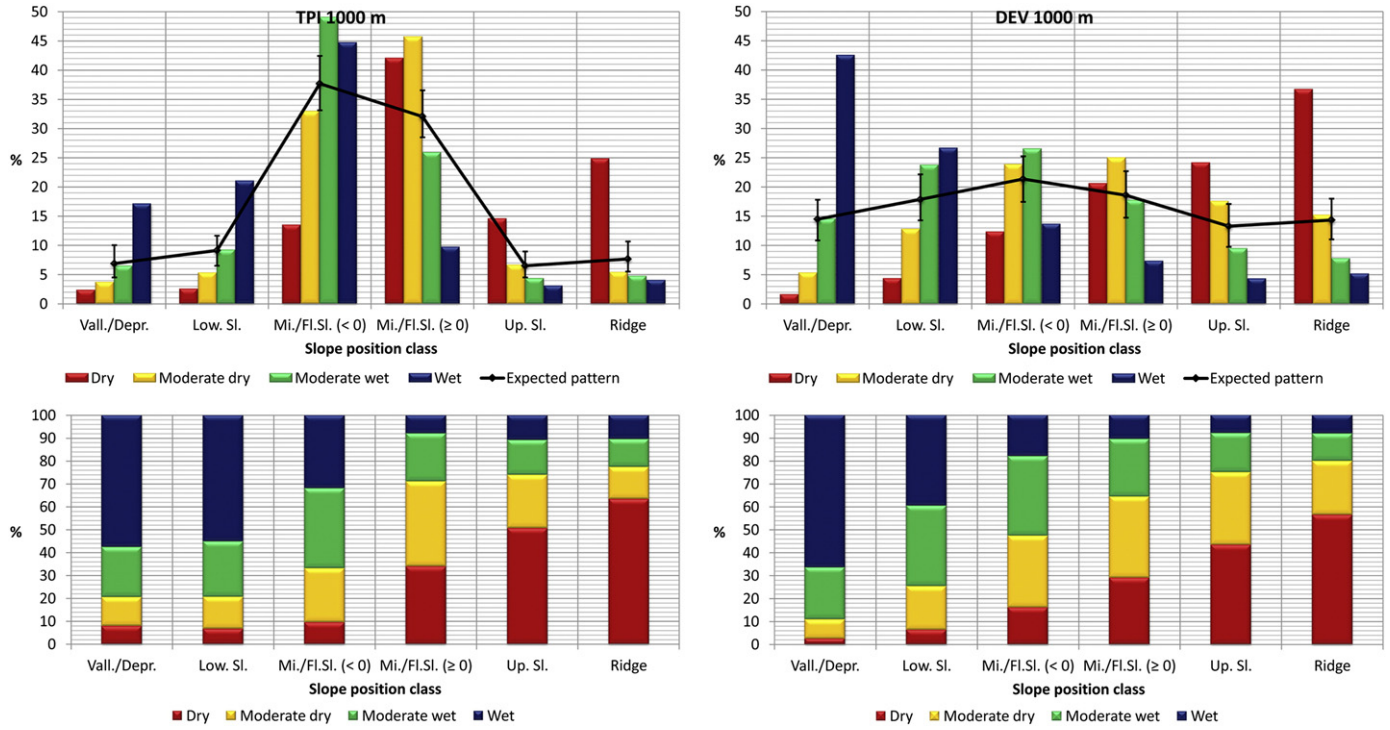

Fig. 10 (*continued*).

depressions were identified in regions characterised by both low and high relief levels.

TPI is an example of a topographic metric that became institutionalised by its integration into widely used tools such as the ESRI products. This resulted not only in the popularity of this metric parameter, but also in the uncritical application by users without a solid geomorphological background. Like other topographic parameters including *DEV*, *TPI* has advantages and disadvantages as well as appropriate and inappropriate uses. This was illustrated by a geoarchaeological study on the distribution of Bronze Age barrows in northwestern Belgium (De Reu et al., 2011; De Reu, 2012). The *TPI* analysis indicated that the barrows were mainly located on middle slopes/flat areas, although they are actually located on higher ridges in an area with a subtle topography (De Reu, 2012). This subtle topography was not recognised using *TPI*. The use of *DEV* corrected this, illustrating that the difference between *TPI* and *DEV* can clearly influence geoarchaeological interpretations.

Although the use of *DEV* provided more realistic landform classifications, there is no definitive DEM-derived map (Pike et al., 2009). Using other parameters such as curvature, aspect, slope, wetness and soil texture along with *DEV* (and/or *TPI*) may lead to better landform classification.

Acknowledgements

We thank the Special Research Fund (BOF) of Ghent University for supporting the integrated project 'Prehistoric Settlement and Land Use Systems in Sandy Flanders (NW Belgium): A Diachronic and Geoarchaeological Approach' (BOF08/GOA/009). Our appreciation also goes to two anonymous reviewers for their helpful and useful comments and suggestions.

References

AGIV, 2001. Bodemkaart (1947–1973). Digitale bodemkaart van het Vlaams Gewest (CD-ROM). Vlaamse Landmaatschappij. Ondersteunend centrum GIS-Vlaanderen, Brussel.
AGIV, 2003. Digitaal hoogtemodel Vlaanderen. Nieuwsbrief GIS-Vlaanderen 16, 3–21.
AGIV, 2004. DHM-Vlaanderen (2001–2004): digitaal hoogtemodel Vlaanderen (CD-ROM). Vlaamse Landmaatschappij. Ondersteunend centrum GIS-Vlaanderen, Brussel.
Berking, J., Beckers, B., Schütt, B., 2010. Runoff in two semi-arid watersheds in a geoarcheological context: a case study of Naga, Sudan, and Resafa, Syria. Geoarchaeology 25, 815–836.
Bevan, A., 2002. The rural landscape of Neopalatial Kythera: a GIS perspective. Journal of Mediterranean Archaeology 15, 217–255.
Bevan, A., Conolly, J., 2004. GIS, archaeological survey, and landscape archaeology on the Island of Kythera, Greece. Journal of Field Archaeology 29, 123–138.
Bolongaro-Crevenna, A., Torres-Rodríguez, V., Sorani, V., Frame, D., Arturo Ortiz, M., 2005. Geomorphometric analysis for characterizing landforms in Morelos State, Mexico. Geomorphology 67, 407–422.
Bue, B.D., Stepinski, T.F., 2006. Automated classification of landforms on Mars. Computers & Geosciences 32, 604–614.
Bunn, A., Hughes, M., Salzer, M., 2011. Topographically modified tree-ring chronologies as a potential means to improve paleoclimate inference. Climatic Change 105, 627–634.
Burrough, P.A., van Gaans, P.F.M., MacMillan, R.A., 2000. High-resolution landform classification using fuzzy k-means. Fuzzy Sets and Systems 113, 37–52.
Christopherson, G.L., 2003. Using ARC/GRID to calculate topographic prominence in an archaeological landscape. ESRI User Conference Proceedings of the 23nd Annual ESRI International User Conference, July 7–11, 2003.
Clark, J.T., Fei, S., Liang, L., Rieske, L.K., 2012. Mapping eastern hemlock: comparing classification techniques to evaluate susceptibility of a fragmented and valued resource to an exotic invader, the hemlock woolly adelgid. Forest Ecology and Management 266, 216–222.
Clennon, J., Kamanga, A., Musapa, M., Shiff, C., Glass, G., 2010. Identifying malaria vector breeding habitats with remote sensing data and terrain-based landscape indices in Zambia. International Journal of Health Geographics 9, 58.
Coulon, A., Morellet, N., Goulard, M., Cargnelutti, B., Angibault, J.-M., Hewison, A.J.M., 2008. Inferring the effects of landscape structure on roe deer (*Capreolus capreolus*) movements using a step selection function. Landscape Ecology 23, 603–614.
Crombé, P., Sergant, J., Robinson, E., De Reu, J., 2011. Hunter-gatherer responses to environmental change during the Pleistocene–Holocene transition in the southern North Sea basin: final Palaeolithic–final Mesolithic land use in northwest Belgium. Journal of Anthropological Archaeology 30, 454–471.
de la Giroday, H.-M., Carroll, A., Lindgren, B., Aukema, B., 2011. Incoming! Association of landscape features with dispersing mountain pine beetle populations during a range expansion event in western Canada. Landscape Ecology 26, 1097–1110.
De Moor, G., Heyse, I., 1978. De morfologische evolutie van de Vlaamse vallei. De Aardrijkskunde 4, 343–375.
De Reu, J., 2012. Land of the Dead. A Comprehensive Study of the Bronze Age Burial Landscape in North-western Belgium. University Press, Zelzate.
De Reu, J., Bourgeois, J., De Smedt, P., Zwertvaegher, A., Antrop, M., Bats, M., De Maeyer, P., Finke, P., Van Meirvenne, M., Verniers, J., Crombé, P., 2011. Measuring the relative topographic position of archaeological sites in the landscape, a case study on the Bronze Age barrows in northwest Belgium. Journal of Archaeological Science 38, 3435–3446.

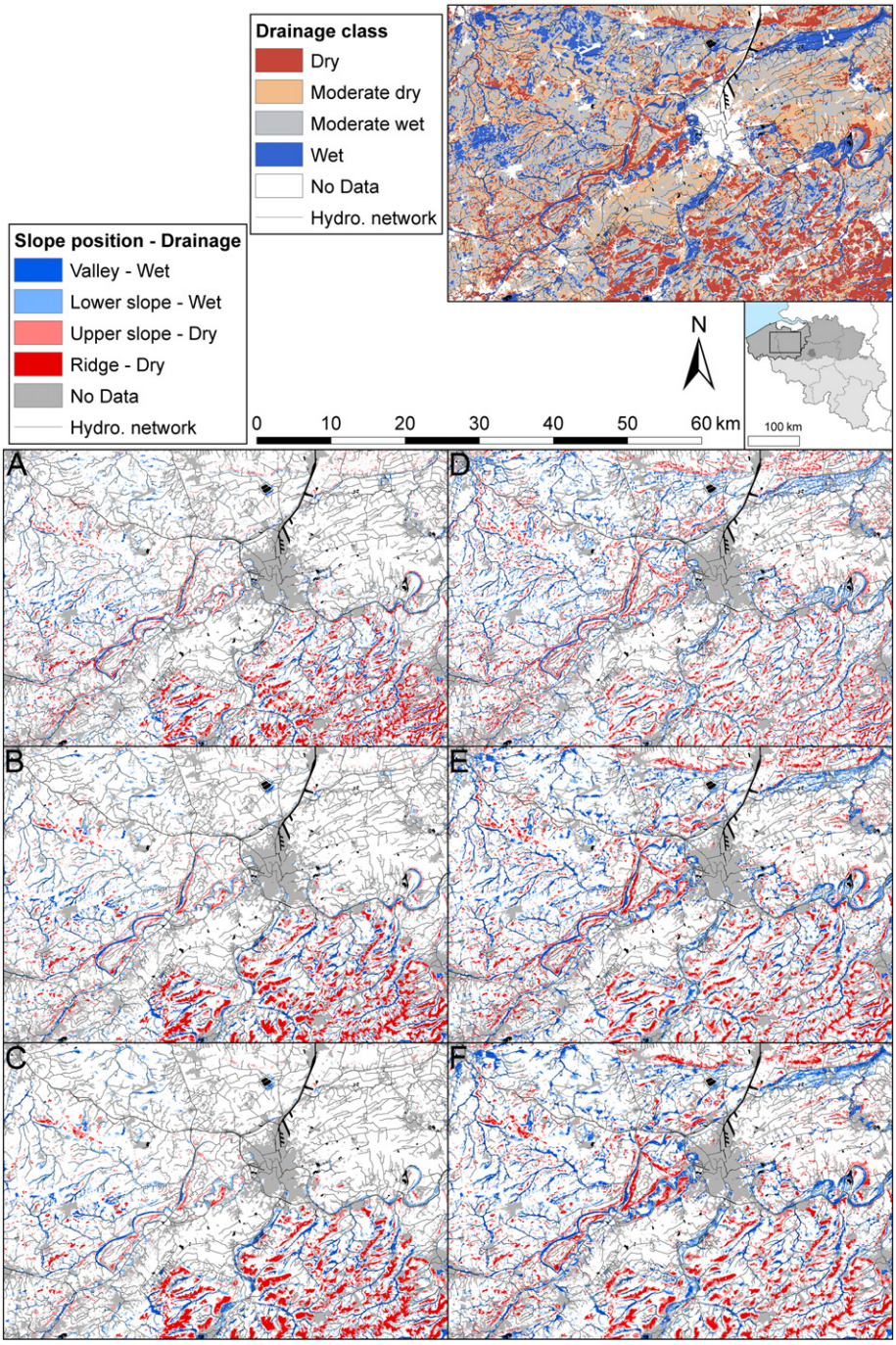

Fig. 11. Spatial relation among the drainage classes, hydrological networks and slope position classes based on *DEV* or *TPI* for different neighbourhood sizes (300, 600 and 1000 m). (A) *DEV*, 300 m. (B) *DEV*, 600 m. (C) *DEV*, 1000 m. (D) *TPI*, 300 m. (E) *TPI*, 600 m. (F) *TPI*, 1000 m.

Deng, Y., 2007. New trends in digital terrain analysis: landform definition, representation, and classification. Progress in Physical Geography 31, 405–419.
Deumlich, D., Schmidt, R., Sommer, M., 2010. A multiscale soil–landform relationship in the glacial-drift area based on digital terrain analysis and soil attributes. Journal of Plant Nutrition and Soil Science 173, 843–851.
Drăguț, L., Blaschke, T., 2006. Automated classification of landform elements using object-based image analysis. Geomorphology 81, 330–344.
Etienne, C., Lehmann, A., Goyette, S., Lopez-Moreno, J.-I., Beniston, M., 2010. Spatial predictions of extreme wind speeds over Switzerland using generalized additive models. Journal of Applied Meteorology and Climatology 49, 1956–1970.
Fairén-Jiménez, S., 2007. British Neolithic rock art in its landscape. Journal of Field Archaeology 32, 283–295.
Fei, S., Schibig, J., Vance, M., 2007. Spatial habitat modeling of American chestnut at Mammoth Cave National Park. Forest Ecology and Management 252, 201–207.
Francés, A.P., Lubczynski, M.W., 2011. Topsoil thickness prediction at the catchment scale by integration of invasive sampling, surface geophysics, remote sensing and statistical modeling. Journal of Hydrology 405, 31–47.
Gallant, J.C., Wilson, J.P., 2000. Primary topographic attributes. In: Wilson, J.P., Gallant, J.C. (Eds.), Terrain Analysis: Principles and Applications. Wiley, New York, pp. 51–85.
Giles, P.T., 1998. Geomorphological signatures: classification of aggregated slope unit objects from digital elevation and remote sensing data. Earth Surface Processes and Landforms 23, 581–594.
Giorgis, M., Tecco, P., Cingolani, A., Renison, D., Marcora, P., Paiaro, V., 2011. Factors associated with woody alien species distribution in a newly invaded mountain system of central Argentina. Biological Invasions 13, 1423–1434.
Grohmann, C.H., Riccomini, C., 2009. Comparison of roving-window and search-window techniques for characterising landscape morphometry. Computers & Geosciences 35, 2164–2169.
Guisan, A., Weiss, S.B., Weiss, A.D., 1999. GLM versus CCA spatial modeling of plant species distribution. Plant Ecology 143, 107–122.
Han, H., Jang, K., Song, J., Seol, A., Chung, W., Chung, J., 2011. The effects of site factors on herb species diversity in Kwangneung forest stands. Forest Science and Technology 7, 1–7.

Hengl, T., Reuter, H.I. (Eds.), 2009. Geomorphometry: concepts, software, applications. Developments in Soil Science, 33. Elsevier, Amsterdam.
Hengl, T., Rossiter, D.G., 2003. Supervised landform classification to enhance and replace photo-interpretation in semi-detailed soil survey. Soil Science Society of America Journal 67, 1810–1822.
Heyse, I., 1979. Bijdrage tot de geomorfologische kennis van het noordwesten van Oost-Vlaanderen (België). Verhandelingen van de Koninklijke Academie voor Wetenschappen, Letteren en Schone Kunsten van België. Klasse der wetenschappen, 155. Paleis der Academiën, Brussel.
Iampietro, P.J., Kvitek, R.G., Morris, E., 2005. Recent advances in automated genus-specific marine habitat mapping enabled by high-resolution multibeam bathymetry. Marine Technology Society Journal 39, 83–93.
Illés, G., Kovács, G., Heil, B., 2011. Comparing and evaluating digital soil mapping methods in a Hungarian forest reserve. Canadian Journal of Soil Science 91, 615–626.
Irvin, B.J., Ventura, S.J., Slater, B.K., 1997. Fuzzy and isodata classification of landform elements from digital terrain data in Pleasant Valley, Wisconsin. Geoderma 77, 137–154.
Iwahashi, J., Pike, R.J., 2007. Automated classifications of topography from DEMs by an unsupervised nested-means algorithm and a three-part geometric signature. Geomorphology 86, 409–440.
Jenness, J., 2006. Topographic Position Index (tpi_jen.avx) Extension for ArcView 3.x, v. 1.3a. Jenness Enterprises.
Kvamme, K.L., 1992. Terrain form analysis of archaeological location through geographic information systems. In: Lock, G., Moffett, J. (Eds.), Computer Applications and Quantitative Methods in Archaeology 1991. : BAR International Series. Tempus Reparatum, Oxford, pp. 127–136.
Lacki, M.J., Cox, D.R., Dodd, L.E., Dickinson, M.B., 2009. Response of northern bats (*Myotis septentrionalis*) to prescribed fires in eastern Kentucky forests. Journal of Mammalogy 90, 1165–1175.
Lesschen, J.P., Kok, K., Verburg, P.H., Cammeraat, L.H., 2007. Identification of vulnerable areas for gully erosion under different scenarios of land abandonment in southeast Spain. Catena 71, 110–121.
Liu, M., Hu, Y., Chang, Y., He, X., Zhang, W., 2009. Land use and land cover change analysis and prediction in the upper reaches of the Minjiang River, China. Environmental Management 43, 899–907.
Liu, H., Bu, R., Liu, J., Leng, W., Hu, Y., Yang, L., Liu, H., 2011. Predicting the wetland distributions under climate warming in the Great Xing'an Mountains, northeastern China. Ecological Research 26, 605–613.
Llobera, M., 2001. Building past landscape perception with GIS: understanding topographic prominence. Journal of Archaeological Science 28, 1005–1014.
Lundblad, E.R., Wright, D.J., Miller, J., Larkin, E.M., Rinehart, R., Naar, D.F., Donahue, B.T., Anderson, S.M., Battista, T., 2006. A benthic terrain classification scheme for American Samoa. Marine Geodesy 29, 89–111.
MacMillan, R.A., Pettapiece, W.W., Nolan, S.C., Goddard, T.W., 2000. A generic procedure for automatically segmenting landforms into landform elements using DEMs, heuristic rules and fuzzy logic. Fuzzy Sets and Systems 113, 81–109.
MacMillan, R.A., Jones, R.K., McNabb, D.H., 2004. Defining a hierarchy of spatial entities for environmental analysis and modeling using digital elevation models (DEMs). Computers, Environment and Urban Systems 28, 175–200.
McGarigal, K., Tagil, S., Cushman, S., 2009. Surface metrics: an alternative to patch metrics for the quantification of landscape structure. Landscape Ecology 24, 433–450.
Miliaresis, G.C., Argialas, D.P., 1999. Segmentation of physiographic features from the global digital elevation model/GTOPO30. Computers & Geosciences 25, 715–728.
Mora-Vallejo, A., Claessens, L., Stoorvogel, J., Heuvelink, G.B.M., 2008. Small scale digital soil mapping in southeastern Kenya. Catena 76, 44–53.
Moss, W., Hamapumbu, H., Kobayashi, T., Shields, T., Kamanga, A., Clennon, J., Mharakurwa, S., Thuma, P., Glass, G., 2011. Use of remote sensing to identify spatial risk factors for malaria in a region of declining transmission: a cross-sectional and longitudinal community survey. Malaria Journal 10, 163.
Patterson, J.J., 2008. Late Holocene land use in the Nutzotin Mountains: lithic scatters, viewsheds, and resource distribution. Arctic Anthropology 45, 114–127.
Pike, R.J., Evans, A.A., Hengl, T., 2009. Geomorphometry: a brief guide. In: Hengl, T., Reuter, H.I. (Eds.), Geomorphometry. Concepts, Software, Applications. Developments in Soil Science. Elsevier, Amsterdam, pp. 3–30.
Pinard, V., Dussault, C., Ouellet, J.-P., Fortin, D., Courtois, R., 2012. Calving rate, calf survival rate, and habitat selection of forest-dwelling caribou in a highly managed landscape. Journal of Wildlife Management 76, 189–199.
Platt, R.V., Schoennagel, T., Veblen, T.T., Sherriff, R.L., 2011. Modeling wildfire potential in residential parcels: a case study of the north-central Colorado Front Range. Landscape and Urban Planning 102, 117–126.
Podchong, S., Schmidt-Vogt, D., Honda, K., 2009. An improved approach for identifying suitable habitat of Sambar Deer (*Cervus unicolor* Kerr) using ecological niche analysis and environmental categorization: case study at Phu-Khieo Wildlife Sanctuary, Thailand. Ecological Modelling 220, 2103–2114.
Pracilio, G., Smettem, K., Bennett, D., Harper, R., Adams, M., 2006. Site assessment of a woody crop where a shallow hardpan soil layer constrained plant growth. Plant and Soil 288, 113–125.
Prima, O.D.A., Echigo, A., Yokoyama, R., Yoshida, T., 2006. Supervised landform classification of northeast Honshu from DEM-derived thematic maps. Geomorphology 78, 373–386.
Reuter, H.I., Nelson, A., 2009. Geomorphometry in ESRI packages. In: Hengl, T., Reuter, H.I. (Eds.), Geomorphometry. Concepts, Software, Applications. : Developments in Soil Science. Elsevier, Amsterdam, pp. 269–291.
Roughley, C., 2001. Understanding the Neolithic landscape of the Carnac region: a GIS approach. In: Stancic, Z., Veljanovski, T. (Eds.), Computing Archaeology for Understanding the Past — CAA 2000 — Computer Applications and Quantitative Methods in Archaeology. : Proceedings of the 28th Conference, Ljubljana, April 2000. BAR International Series. Archaeopress, Oxford, pp. 211–218.
Schmidt, J., Dikau, R., 1999. Extracting geomorphometric attributes and objects from digital elevation models — semantics, methods, and future needs. In: Dikau, R., Sourer, H. (Eds.), GIS for Earth Surface Systems: Analysis and Modelling of the Natural Environment. Gebrüder Borntraeger, Berlin, pp. 153–173.
Squires, J.R., Decesare, N.J., Kolbe, J.A., Ruggiero, L.F., 2008. Hierarchical den selection of Canada lynx in western Montana. Journal of Wildlife Management 72, 1497–1506.
Tagil, S., Jenness, J., 2008. GIS-based automated landform classification and topographic, landcover and geologic attributes of landforms around the Yazoren Polje, Turkey. Journal of Applied Sciences 8, 910–921.
Tilley, C., 1994. A Phenomenology of Landscape: Places, Paths and Monuments. Berg, Oxford.
Verfaillie, E., Van Lancker, V., Van Meirvenne, M., 2006. Multivariate geostatistics for the predictive modelling of the surficial sand distribution in shelf seas. Continental Shelf Research 26, 2454–2468.
Warren, R.E., Asch, D.L., 2000. A predictive model of archaeological site location in the eastern Prairie Peninsula. In: Wescott, K.L., Brandon, R.J. (Eds.), Practical Applications of GIS for Archaeologists. A Predictive Modeling Toolkit. Taylor & Francis, London, pp. 3–32.
Weber, T.C., 2011. Maximum entropy modeling of mature hardwood forest distribution in four U.S. states. Forest Ecology and Management 261, 779–788.
Weiss, A.D., 2001. Topographic position and landforms analysis. Poster Presentation, ESRI Users Conference, San Diego, CA.
Werbrouck, I., Antrop, M., Van Eetvelde, V., Stal, C., De Maeyer, P., Bats, M., Bourgeois, J., Court-Picon, M., Crombé, P., De Reu, J., De Smedt, P., Finke, P.A., Van Meirvenne, M., Verniers, J., Zwertvaegher, A., 2011. Digital elevation model generation for historical landscape analysis based on LiDAR data, a case study in Flanders (Belgium). Expert Systems with Applications 38, 8178–8185.
Wilson, M.F.J., O'Connell, B., Brown, C., Guinan, J.C., Grehan, A.J., 2007. Multiscale terrain analysis of multibeam bathymetry data for habitat mapping on the continental slope. Marine Geodesy 30, 3–35.
Wood, S.W., Murphy, B.P., Bowman, D.M.J.S., 2011. Firescape ecology: how topography determines the contrasting distribution of fire and rain forest in the south-west of the Tasmanian Wilderness World Heritage Area. Journal of Biogeography 38, 1807–1820.
Wright, D.J., Heyman, W.D., 2008. Introduction to the special issue: marine and coastal GIS for geomorphology, habitat mapping, and marine reserves. Marine Geodesy 31, 223–230.
Young, M.A., Kvitek, R.G., Iampietro, P.J., Garza, C.D., Maillet, R., Hanlon, R.T., 2011. Seafloor mapping and landscape ecology analyses used to monitor variations in spawning site preference and benthic egg mop abundance for the California market squid (*Doryteuthis opalescens*). Journal of Experimental Marine Biology and Ecology 407, 226–233.
Zhang, Y., He, H., Dijak, W., Yang, J., Shifley, S., Palik, B., 2009. Integration of satellite imagery and forest inventory in mapping dominant and associated species at a regional scale. Environmental Management 44, 312–323.
Zieger, S., Stieglitz, T., Kininmonth, S., 2009. Mapping reef features from multibeam sonar data using multiscale morphometric analysis. Marine Geology 264, 209–217.